Continuous-wave ultraviolet laser action in strongly scattering Nd-doped alumina

B. Li, G. Williams, and S. C. Rand

Division of Applied Physics, Randall Laboratory, University of Michigan, Ann Arbor, Michigan 48109–1022

T. Hinklin and R. M. Laine

Department of Materials Science & Engineering, University of Michigan, Ann Arbor, Michigan 48109

Received September 17, 2001

We report electrically pumped, cw laser action near 405 nm from Nd^{3+}-doped δ-alumina nanopowders. To our knowledge, this is the first report of stimulated emission from the high-lying ^2F-excited states, achieved through feedback from strong elastic scattering of light over transport path lengths shorter than half a wavelength. © 2002 Optical Society of America

OCIS codes: 140.0140, 140.5680, 140.3610.

Nd solid-state lasers customarily operate on the $^4F_{3/2}$–$^4I_{11/2}$ transition of the Nd^{3+} ion and provide reliable sources for metrology, quantum optics, high-field studies, high-power industrial, and other applications. For infrared operation, Nd lasers are sustained by population inversion of a relatively low energy state that is easily excited by flash lamps or diodes. Operation at shorter wavelengths has been reported through the use of internal doubling[1] and upconversion,[2] but to our knowledge laser action from the long-lived, high-lying ^2F levels located above $38,000\ cm^{-1}$ has never been reported, because of the difficulty of pumping them efficiently. Inversion of these levels opens up new possibilities, however, for visible and ultraviolet sources based on Nd^{3+}. Here we report continuous-wave laser action near 405 nm from the $^2F_{5/2}$ level of Nd^{3+} in δ-Al_2O_3 nanopowders as well as advances in the use of electrical pumping and strong electromagnetic localization[3,4] that yield continuous nanoscopic laser action in a dielectric host without any external feedback structure.

Highly scattering powders are difficult to pump optically because incident light does not penetrate the medium well, particularly in the regime of strongly localized electromagnetic transport, when the attenuation distance is less than a wavelength (λ). Then, irrespective of incident intensity, light penetrates a short, fixed distance ($\sim\lambda$) below the surface and is almost entirely reflected. Instead, we used electron pumping to energize high-lying states of Nd^{3+} in strong scattering dielectric powders. Electrons have penetration depths that are voltage dependent and typically exceed an optical wavelength in the range 1–10 keV. Hence they offer control over the positioning of the pumped volume with respect to the surface of the medium. In this Letter we show that mild electron excitation in doped oxide nanocrystals readily generates continuous stimulated emission at room temperature in samples that are free of absorption and yet have transport mean free paths shorter than $\lambda/2$.

Our samples consisted of unaggregated, single-crystal δ-alumina particles[5–7] with a dopant level of 1000 parts in 10^6 (ppm) Nd^{3+} ions. The size distribution was log normal, with 240 Nd^{3+} ions per particle of mean diameter 27 nm. Powders were packed (at ~30 psi) into the recesses of an oxygen-free copper platen in an ultrahigh-vacuum chamber at $<10^{-9}$ Torr. A steerable beam of 2–10-keV electrons was lightly focused to a spot diameter of 1–2 mm on the sample. Luminescence was analyzed with a 1-m Czerny–Turner grating spectrometer. The beam current was monitored with a Faraday cup and precisely controlled with a calibrated grid voltage, yielding fluctuations of less than 1%/h and long-term reproducibility better than 3%.

Cathodoluminescence (CL) spectra, recorded for various beam currents and voltages in as-prepared powder samples, were helpful in assigning Nd^{3+} $4f$–$4f$ transitions and quenching dynamics, which are essential for understanding the mechanism of light emission. In Fig. 1, two spectra are shown at different currents in one sample. At 3.3 μA, the largest peaks in the spectrum occur above $25,000\ cm^{-1}$. At 16.9 μA the largest peaks appear below $25,000\ cm^{-1}$ and the original intense lines have vanished. Such dramatic spectral quenching is unexpected in phosphors and is difficult to understand without detailed transition assignments. Spectroscopic studies of RE^{3+}:δ–Al_2O_3 were not possible in the past, owing to the difficulty of preparing doped, δ-phase crystals by traditional growth methods. This forced us to make assignments in the powders by other means. RE^{3+} emission wavelengths can be predicted within a few nanometers in most materials,[8]

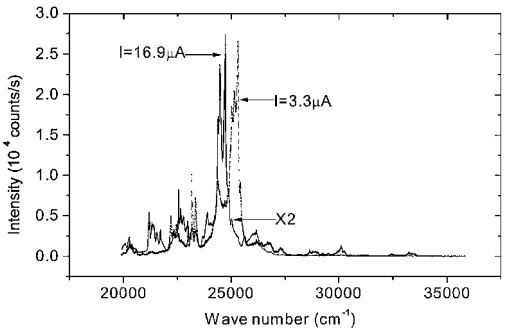

Fig. 1. CL spectra of Nd:δ – Al_2O_3 nanoparticles (ϕ = 27 nm) at I = 3.3 μA and I = 16.9 μA at 8 kV, showing intensity reversals near $25,000\ cm^{-1}$.

0146-9592/02/060394-03$15.00/0

but confusion with overlapping transitions can be avoided only by precise determination of additional characteristics or splittings, for example, the interval between the $^2F_{5/2}$ and $^2F_{7/2}$ multiplets. An important determination of this type can be made by observation of cathodoluminescent transitions from $^2F_{5/2}$ and $^2F_{7/2}$ levels to one and the same state, for instance, singlet state $^2P_{1/2}$ (Fig. 2). ^2F–$^2P_{1/2}$ transitions can be identified by comparison of CL with photoluminescence spectra obtained by use of UV excitation at 363 nm that generates emission lines from all the radiative states lying below the ^2F multiplets. Emission features that appear in CL but not in photoluminescence can then confidently be assigned as ^2F emissions. Because Nd is Kramers degenerate, its Stark sublevels are $[J + (1/2)]$ degenerate, so three $^2F_{5/2}$–$^2P_{1/2}$ transitions to the long-wavelength side of 660 nm and four $^2F_{7/2}$–$^2P_{1/2}$ transitions to the short-wavelength side are expected. The figure shows how observation of all seven features, especially the lowest energy features of each set, reveals the interval Δ between the $^2F_{5/2}$ and $^2F_{7/2}$ multiplets. The value determined from the $^2P_{1/2}$ features is $\Delta = 644 \pm 15\ \mathrm{cm}^{-1}$.

In Fig. 3 we note that near $25,000\ \mathrm{cm}^{-1}$, where the $^2F_{5/2}$–$^4F_{9/2}$, $^2F_{5/2}$–$^4F_{7/2}$ and $^2F_{7/2}$–$^4F_{9/2}$ transitions are expected, the $^2F_{5/2}$–$^2F_{7/2}$ interval occurs again. In this range the observed interval is $\Delta' = 664 \pm 15\ \mathrm{cm}^{-1}$, so that $\Delta = \Delta'$ within experimental error. Although we cannot rule out assignments of some lines above $25,000\ \mathrm{cm}^{-1}$ to $^2F_{5/2}$–$^4F_{7/2}$, the correspondence between these intervals provides independent corroboration that the upper levels of all the emission features in Fig. 3 are indeed $^2F_{5/2}$ or $^2F_{7/2}$. A plot of the luminescent intensities observed on transitions from either of these two high-lying multiplets (where unambiguous assignments can be made) as a function of beam current is presented in Fig. 4. Note that, regardless of which ^2F multiplet is the upper state, all visible and UV ^2F transitions quench rapidly at the threshold current of ~3.5 μA, except one. The fact that $^2F_{7/2}$ transitions quench when $^2F_{5/2}$ transitions do should not be too surprising, since the Boltzmann factor ($\exp(-\hbar\Delta/k_BT) \sim 0.04$ at room temperature) for occupation of the upper multiplet is significant, causing its population to be proportional to that of $^2F_{5/2}$. However, the observation that the $^2F_{5/2}$–$^4F_{9/2}$ transition grows above a well-defined threshold current while the intensities on other transitions from the same initial upper state (or its thermally connected companion) vanish is uniquely attributable to stimulated emission. Only stimulated emission can alter the effective branching ratios for radiative decay from a single level to several others. Consequently, Figs. 3 and 4 provide compelling evidence for stimulated emission at 409.6, 408.1, and 404.1 nm above ~4 μA.

An important aspect of the current dependence of intensity on the $^2F_{5/2}$–$^4F_{9/2}$ transition (Fig. 4) is its linearity above threshold. At 3.5 μA, the intensity of this line begins to increase linearly until it saturates near 12 μA. Linearity is characteristic of oscillators, whereas exponential growth typifies amplifiers. This reveals that very effective feedback assists in the attainment of threshold in our samples. Theoretically, feedback may arise from internal reflection at the vacuum–powder interface (a one-mirror laser), from reflection among particles located on a macroscopic closed path (ring laser), or from strong multiple scattering (localization). However, Figs. 3 and 5 show that, when electrons activate ions at depths greater than the transport distance of light, emission increases and threshold decreases. This improvement in laser characteristics as the gain

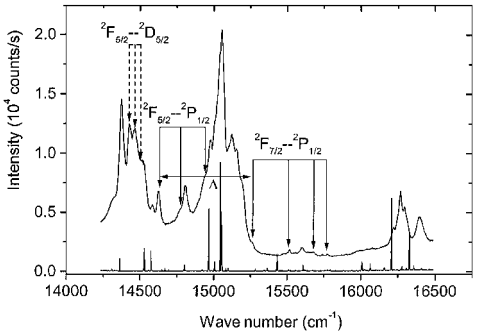

Fig. 2. Identification of ^2F emissions to singlet state $^2P_{1/2}$ of Nd^{3+}. Top curve, CL including ^2F multiplet emission; bottom curve, photoluminescence excluding ^2F emission.

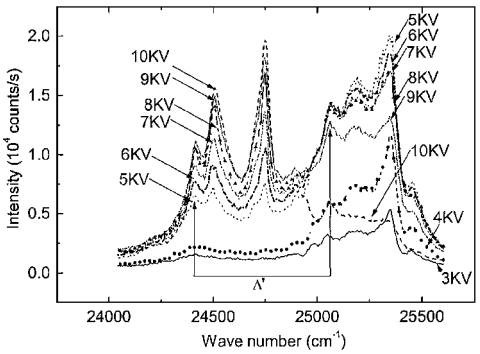

Fig. 3. Voltage dependence of CL spectral peaks in the $25,000$-cm^{-1} region. Features above $25,000\ \mathrm{cm}^{-1}$ grow rapidly up to 5 kV and then quench. Features below $25,000\ \mathrm{cm}^{-1}$ are absent until 5 kV. The splitting between these groups is labeled Δ'.

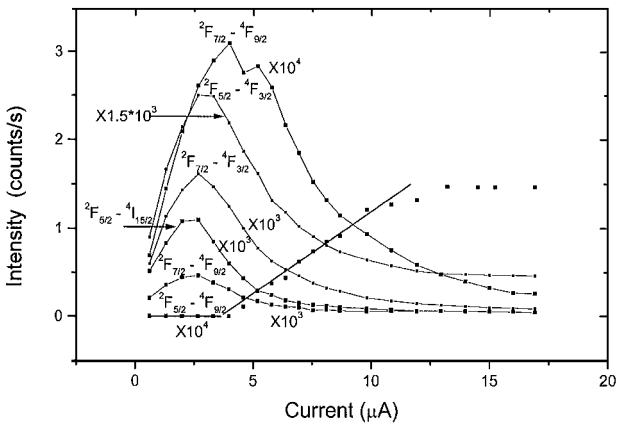

Fig. 4. Current dependence of ultraviolet and visible CL intensities of the $^2F_{5/2}$ and $^2F_{7/2}$ states at 8 kV. All curves (but one) quench rapidly above 3 μA, where intensity on the $^2F_{5/2}$–$^4F_{9/2}$ transition undergoes an abrupt change in slope.

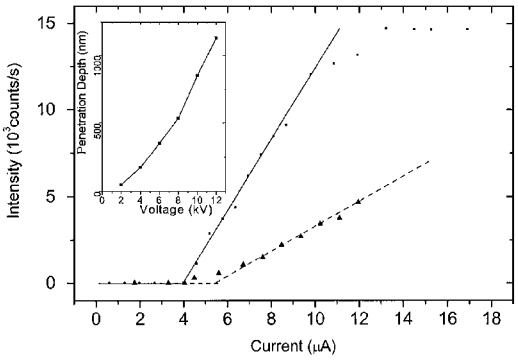

Fig. 5. Luminescent output at 4 and 8 kV in Nd:$\delta - Al_2O_3$. The current range is greater at 8 kV than at 4 kV because of extended linear grid control. Inset, penetration depth versus voltage, calculated with a low-energy Monte Carlo routine.

volume recedes (by several attenuation lengths) below the surface indicates that surface reflection cannot account for the feedback. Since the particles are less than $\lambda/15$ in diameter and are densely packed, it is also evident that morphological resonances cannot provide efficient feedback. Unlike earlier experiments in which mode structure and coherence of pulsed powder lasers were reported,[9–11] our observations are not consistent with light propagation around a closed path. As we discuss below, however, the possibility that multiple scattering gives rise to a nonpropagating, stimulated field through strong localization is entirely consistent with our observations.

Scattering conditions were evaluated by coherent backscattering (CBS) techniques and have been reported elsewhere,[6] so we only summarize key results here. First, CBS data from our samples showed a broad backscattering cone, as expected for small particles with a short mean free transport length, l^*. We deduced a value of $l^* = 174 \pm 31$ nm, using standard analysis at $\lambda = 488$ nm.[12] This value is somewhat less than $\lambda/2$. Second, the CBS cusp was triangular at small angles. This permitted us to estimate a limit for losses in terms of a characteristic absorption length, $l_\alpha > 1$ cm.

The observations of spectral quenching (Figs. 1 and 3), emission thresholding, and linear output above threshold (Fig. 4) collectively furnish clear evidence of Nd^{3+}-laser action in the 4–10-keV range. Since conventional cavities support cw laser action only with high-reflectivity mirrors, these observations alone imply that light experiences high reflectivity in all directions within our samples. However, this point is made more forcefully by our CBS measurements, which show that light in our samples propagates forward less than half a wavelength regardless of direction or polarization. Given that the coherence length is limited to a subwavelength value $l_c < l^* < \lambda$ in the absence of significant absorption ($\lambda \ll l_\alpha$), light generated by impurity ions within our powders necessarily[13] acquires a spatial distribution resembling that of a three-dimensional evanescent wave.

We conclude that laser action in our samples results from strong localization. In our experiments, emission is evidently stimulated coherently over distance scales of tens of nanometers, but spatial randomization on length scales of $\lambda/2$ or more precludes directionality or mode selectivity. Backscattered light (and laser output) in our experiments is nearly speckle free, consistent with a subwavelength effective coherence length. All frequencies within the luminescent linewidth experience comparable gain and feedback, independently of observation angle, just as expected for continuous, truly random laser action. Our experiments demonstrate cw laser action at new wavelengths near 405 nm in Nd^{3+}-doped nanopowder at room temperature for what is to our knowledge the first time. The mild electrical pumping conditions necessary to achieve this result lend support to the idea that the threshold for laser action is lowered by the onset of strong scattering. We reached similar conclusions earlier for Pr^{3+}- and Ce^{3+}-doped powders,[6] at visible and ultraviolet wavelengths, making it apparent that doped, dielectric nanophosphors may provide an entire family of bright omnidirectional, speckle-free, monochromatic sources for improved lighting, chemical sensors, displays, short-range aircraft or space communication, nanoscale lithography, and other applications.

The authors gratefully acknowledge research support from the U.S. Air Force Office of Scientific Research (F49620-99-1-0158), the National Science Foundation and DMR 9975542), and the Army Research Office (DAAD 19-99-1-0229). Monte Carlo calculations of electron penetration were performed by H.-Y. Chan. S. C. Rand's e-mail address is scr@eecs.umich.edu.

References

1. T. Y. Fan, A. Cordova-Plaza, M. J. F. Digonnet, R. L. Byer, and H. J. Shaw, J. Opt. Soc. Am. B **3,** 140 (1986).
2. R. M. Macfarlane, F. Tong, A. J. Silversmith, and W. Lenth, Appl. Phys. Lett. **52,** 1300 (1988).
3. S. John, Phys. Rev. Lett. **53,** 2169 (1984).
4. P. W. Anderson, Philos. Mag. B **52,** 505 (1985).
5. G. Williams, S. C. Rand, T. Hinklin, and R. M. Laine, in *Conference on Lasers and Electro-Optics (CLEO/US)* (Optical Society of America, Washington, D.C., 1999), paper CTuG5.
6. G. R. Williams, B. Bayram, S. C. Rand, T. Hinklin, and R. M. Laine, Phys. Rev. A **65,** 013807 (2001).
7. R. M. Laine, T. Hinklin, G. Williams, and S. C. Rand, Mater. Sci. Forum **344–346,** 500 (2000).
8. C. Gorller-Walrand and K. Binnenans, in *Spectral Intensities of $f-f$ Transitions*, K. A. Gschneidner and L. Eyring, eds., Vol. 25 of Handbook of Physics and Chemistry of Rare Earths (Elsevier, New York, 1998), pp. 101–264.
9. H. Cao, Y. G. Zhao, S. T. Ho, E. W. Seelig, Q. H. Wang, and R. P. H. Chang, Phys. Rev. Lett. **82,** 2278 (1999).
10. H. Cao, Y. Ling, J. Y. Xu, C. Q. Cao, and P. Kumar, Phys. Rev. Lett. **86,** 4524 (2001).
11. R. K. Thareja and A. Mitra, Appl. Phys. B **71,** 181 (2000).
12. J. X. Zhu, D. J. Pine, and D. A. Weitz, Phys. Rev. A **44,** 3948 (1991).
13. J. W. Goodman, *Statistical Optics* (Wiley, New York, 1985), p. 206.